Boise State University
ScholarWorks

CGISS Publications and Presentations

Center for Geophysical Investigation of the Shallow Subsurface (CGISS)

7-11-2007

Transient Storage as a Function of Geomorphology, Discharge, and Permafrost Active Layer Conditions in Arctic Tundra Streams

Jay P. Zarnetske
Utah State University

Michael N. Gooseff
Colorado School of Mines

Troy R. Brosten
Boise State University

John H. Bradford
Boise State University

James P. McNamara
Boise State University

See next page for additional authors

Authors

Jay P. Zarnetske, Michael N. Gooseff, Troy R. Brosten, John H. Bradford, James P. McNamara, and W. Breck Bowden

Click Here for Full Article

Transient storage as a function of geomorphology, discharge, and permafrost active layer conditions in Arctic tundra streams

Jay P. Zarnetske,[1,2] Michael N. Gooseff,[3] Troy R. Brosten,[4] John H. Bradford,[4] James P. McNamara,[4] and W. Breck Bowden[5]

[1]   Transient storage of solutes in hyporheic zones or other slow-moving stream waters plays an important role in the biogeochemical processes of streams. While numerous studies have reported a wide range of parameter values from simulations of transient storage, little field work has been done to investigate the correlations between these parameters and shifts in surface and subsurface flow conditions. In this investigation we use the stream properties of the Arctic (namely, highly varied discharges, channel morphologies, and subchannel permafrost conditions) to isolate the effects of discharge, channel morphology, and potential size of the hyporheic zone on transient storage. We repeated stream tracer experiments in five morphologically diverse tundra streams in Arctic Alaska during the thaw season (May–August) of 2004 to assess transient storage and hydrologic characteristics. We compared transient storage model parameters to discharge (Q), the Darcy-Weisbach friction factor (f), and unit stream power (ω). Across all studied streams, permafrost active layer depths (i.e., the potential extent of the hyporheic zone) increased throughout the thaw season, and discharges and velocities varied dramatically with minimum ranges of eight-fold and four-fold, respectively. In all reaches the mean storage residence time (t_{stor}) decreased exponentially with increasing Q, but did not clearly relate to permafrost active layer depths. Furthermore, we found that modeled transient storage metrics (i.e., t_{stor}, storage zone exchange rate (α_{OTIS}), and hydraulic retention (R_h)) correlated better with channel hydraulic descriptors such as f and ω than they did with Q or channel slope. Our results indicate that Q is the first-order control on transient storage dynamics of these streams, and that f and ω are two relatively simple measures of channel hydraulics that may be important metrics for predicting the response of transient storage to perturbations in discharge and morphology in a given stream.

1. Introduction

1.1. Transient Storage in Streams

[2] Transient storage in streams consists of water connected to the surface flow that is delayed in its downstream transport by a stream feature. Transient storage is controlled by the prevailing physical conditions of the stream, such as discharge, channel structure, and bed composition. Examples of stream features which create transient storage are hyporheic zones or in-channel dead zones created by boulders, constrictions, and vegetation in the main channel [*Harvey and Bencala*, 1993; *Kasahara and Wondzell*, 2003; *Wondzell*, 2006]. In the context of the present study, transient storage refers specifically to the physically retarded (or delayed) fraction of an introduced conservative tracer pulse.

[3] The role of the hyporheic zone in creating transient storage is well documented [e.g., *Harvey and Wagner*, 2000]. Hyporheic flow occurs through the interstitial spaces of channel and bank sediments, which creates a mixing zone of ground and surface waters. The hyporheic zone, like in-channel backwater environments, is a transient storage zone, because it transports water at rates slower than water traveling as surface flow. The diversity of in-channel and hyporheic flow paths and the associated transport times creates a distribution of stream water residence times. This distribution of stream water residence times is important,

---

[1]Department of Watershed Sciences, Utah State University, Logan, Utah, USA.

[2]Now at Department of Geosciences, Oregon State University, Corvallis, Oregon, USA.

[3]Department of Geology and Geological Engineering, Colorado School of Mines, Golden, Colorado, USA.

[4]Department of Geosciences, Boise State University, Boise, Idaho, USA.

[5]Rubenstein School of the Environment and Natural Resources, University of Vermont, Burlington, Vermont, USA.

because it accounts for a substantial proportion of the diverse and intensified biogeochemical activity conditions that exist within watersheds [*Grimm and Fisher*, 1984; *Triska et al.*, 1990; *Findlay et al.*, 1993; *Harvey and Fuller*, 1996].

[4] A substantial amount of research has sought to elucidate the underlying hydrodynamic processes that are responsible for hyporheic exchange and its role in transient storage. Generally, this research was conducted as either field or laboratory based studies with field studies focused on examining the features of the stream-aquifer system that drive exchange, and laboratory studies investigating the fundamental and theoretical processes in detail. Herein, we focus our synthesis of hyporheic understanding on principles derived from field experiments in streams because the present study relies on field investigations. However, for a more extensive discussion of the theoretical and laboratory derived hyporheic principles, see *Packman and Bencala* [2000] and references therein.

[5] Stream feature morphology is an important control on transient storage associated with hyporheic zones [*Harvey and Bencala*, 1993; *Kasahara and Wondzell*, 2003]. As reviewed in *Harvey and Wagner* [2000] and *Packman and Bencala* [2000], the morphologic factors that affect transient storage in hyporheic zones include: channel slope, width, sinuosity and depth of penetration; longitudinal bed morphology; geologic setting and alluvial characteristics; and groundwater aquifer hydraulic properties and geometry. Many of these morphologic hyporheic controls operate on both small and large scales. For example, pressure differentials upstream and downstream of bed features as small as a ripple or as large as a riffle can create a pumping action, which drives hyporheic exchange [e.g., *Packman and Bencala*, 2000]. Additionally, theory and recent laboratory investigations [e.g., *Packman and Salehin*, 2003] suggest that hyporheic exchange is not solely a function of stream morphology, but also a function of flow velocity over a porous bed, and bed permeability. *Packman and Salehin* [2003] demonstrated that the interplay between sediment characteristics and overlying flow conditions plays an important role in hyporheic exchange.

[6] Perturbations in the discharge, elevation of channel stage, and water table also influence overall transient storage [*Pinder and Sauer*, 1971; *D'Angelo et al.*, 1993; *Harvey and Bencala*, 1993; *Morrice et al.*, 1997; *Wörman et al.*, 2002], but the overall understanding of how they correlate to in-channel and hyporheic transient storage dynamics is still unclear. In each of these studies, the extent of the hyporheic flow and associated transient storage increased as stream discharge decreased. Investigations by others [*Legrand-Marcq and Laudelout*, 1985; *Wondzell and Swanson*, 1996] found a somewhat contrary relationship between transient storage and discharge. For example, *Legrand-Marcq and Laudelout* [1985] observed that transient storage was only inversely proportional to discharge over a small range of flows and that it achieved a stable minimum value above certain discharges. This investigation and data from others [*D'Angelo et al.*, 1993; *Morrice et al.*, 1997; *Hart et al.*, 1999] indicate that in-channel transient storage perturbations due to changes in discharge have a greater impact on the overall transient storage of a stream than the influence exerted by the hyporheic zone.

1.2. Transient Storage in Arctic Tundra Streams

[7] Arctic tundra streams underlain by permafrost represent fundamentally simplified surface water-groundwater exchange environments relative to their temperate counterparts. The Arctic streams of this study are generally uninfluenced by large groundwater aquifers and extensive parafluvial exchange due to the presence of permafrost. Because the majority of the transient storage work has occurred in more complex surface water-groundwater stream systems of temperate, and a few tropical and Antarctic environments [e.g., *Morrice et al.*, 1997; *Gooseff et al.*, 2002; *Gucker and Boechat*, 2004] the Arctic stream systems offer an unprecedented opportunity to better isolate the effects of discharge and geomorphology on transient storage in streams. Furthermore, *Edwardson et al.* [2003] provided an initial documentation of transient storage and biogeochemical processing in the hyporheic zones of Arctic tundra streams, in which the hyporheic zones were demonstrated to be significant to the biogeochemical cycling of the streams. Nevertheless, the dynamics of these Arctic hyporheic zones, especially the spatial and temporal extent, are unknown and potentially important.

[8] While transient storage work in Arctic streams has been limited, *Bradford et al.* [2005] recently showed that the active layer of a peat bed Arctic stream was significantly greater than the adjacent terrestrial environs. Here we define active layer as the region of seasonal thaw below the stream channel. This observation by *Bradford et al.* [2005] implies that streams create conditions preferential to a thicker active layer. Overall, the extent of the active layer below Arctic streams is still virtually unknown. The dynamics of active layer growth and how it relates to stream processes are particularly important in light of Arctic climate change, which has increased the duration of the summer thaw season [*Sturm et al.*, 2005]. Furthermore, *Peterson et al.* [1983, 1993] and *Edwardson et al.* [2003] have concluded that the ecological significance of hyporheic zones may be even greater in Arctic environments where nutrient availability is limited.

[9] We hypothesized that within streams underlain by permafrost, the hyporheic zone, including its role in transient storage, is strongly controlled by the extent of ice in the surrounding substrate. Additionally, by conducting transient storage investigations in simplified streams, we set out to explore how transient storage in streams relates to other physical conditions such as morphology and discharge. Thus the primary objective of this study was to correlate the transient storage dynamics (i.e., residence times, storage volumes, and exchange rates) of Arctic streams to several observed physical conditions including discharge, resistance in the open channel, rate of energy expenditure, and active layer extent. Discharge and Darcy-Weisbach friction factor were selected because previous investigations [e.g., *Legrand-Marcq and Laudelout*, 1985; *Hart et al.*, 1999; *Harvey and Wagner*, 2000; *Harvey et al.*, 2003] have correlated these stream characteristics to transient storage conditions. In particular, *Hart et al.* [1999] and *Harvey and Wagner* [2000] found correlations between storage metrics and the friction factor, while *Harvey et al.* [2003] later demonstrated that the friction factor could predict storage characteristics equally well in a stream experiencing changing discharge or changing geomorphology. Stream power
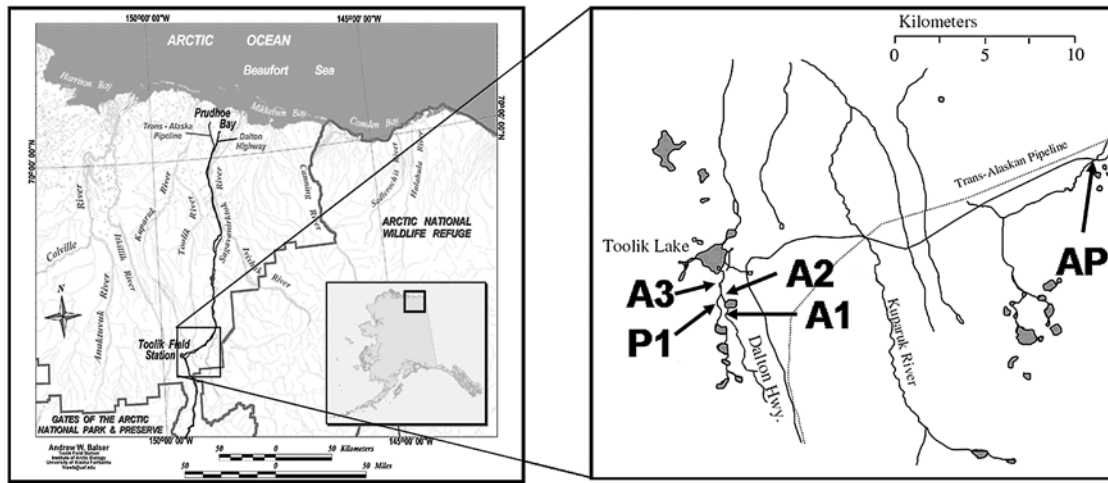
Figure 1. Location of rivers and experimental reaches used in this study (base map modified from http://www.uaf.edu/toolik/gis/ivi_slope_bw.jpg).

per unit of bed width to the best of the authors' knowledge has not been applied in previous transient storage investigations, but was also selected because, like the friction factor, it incorporates both a hydrodynamic (discharge) and morphologic description of streams (slope and width).

2. Study Sites

[10] During the course of this study, we performed experiments on 5 tundra streams located in the northern foothills of Alaska's Brooks Range. Each of the selected streams are in the vicinity of (<20 km from) the Toolik Lake field station (68 38'N, 149 38'W), which is approximately 255 km north of the Arctic Circle and at an average elevation of 720 m above sea level in the foothills province of the Brooks Range (Figure 1). Present river drainages were established following the Wisconsinian glaciation and predominantly exist in glacial outwash valleys [*Hamilton*, 1986]. Vegetation consists primarily of sedges and grasses, mixed with dwarf birch, low willows, and various forbs. The regional hydrology is typified by spring runoff of melting snow initiating a brief active surface flow season between late May and late September [*Kane et al.*, 1991]. Only the largest rivers in the region are capable of maintaining year-round active flow. The region is classified as a high Arctic desert with ~18 cm of rain falling during the thaw season and an additional 10–14 cm of water equivalent falling as snow during the remainder of the year [*McNamara et al.*, 1997]. Thaw season rain events can produce large and localized flashy shifts in stream discharges. With the exception of rare perennial springs, deep groundwater does not associate with surface water, as continuous permafrost can exist up to 300–600 m below the surface [*Osterkamp and Payne*, 1981].

[11] The 5 tundra streams we studied represent the dominant morphotypes of the North Slope: alluvial (A), peat (P), and a combination of these two end-members referred to as alluvial peat (AP) (Table 1). All of these streams are underlain by permafrost, with active layers that initiate and advance rapidly at the beginning of the thaw season, and persist until the end of the thaw season. These active layers achieve depths of >2.0 m beneath alluvial streams and can be less than 0.6 m under peat bed streams [*Bradford et al.*, 2005; *Brosten et al.*, 2006]. The alluvial streams (A1, A2, and A3) are meandering streams with gravel and cobble bed material and planforms similar to temperate mountain environments (e.g., alternating stretches of riffles and pools or step-pool). Stream gradients are relatively steep compared to the other two morphotypes (slopes 0.64–1.18% versus 0.16–0.90%). The peat stream (P1) is a typical beaded stream ("beaded" refers to the large, deep pools connected by short, narrow segments in plan and cross-sectional form), which is formed by preferential thermal erosion [*Péwé*, 1966]. Peat streams are generally low-order streams with peaty channels and have the shallowest slopes and least tendency to meander of the three morphotypes. The alluvial peat stream (AP) represents a morphology that is a combination of alluvial and peat morphotype characteristics. These streams are typified by significant alluvial bed material residing within a larger peat channel. The planform is that of a meandering stream composed from sequences of large pools connected by short, narrow riffles and runs. Discharges for the study streams ranged from 0.05 m^3 s^{-1} in P1 up to 2.7 m^3 s^{-1} in AP during the 2004 thaw season. The ecology of these

Table 1. Characteristics of Arctic Stream Reaches Used in This Study[a]

Study Reach	Stream Name	Reach Length, m From Injection	Morphotype	Substrate	Order	Gradient, %
A1	I8-Inlet	400	Pool-riffle	Cobble	2	0.97
A2	I8-Outlet	250	Pool-riffle	Cobble	2	1.18
A3	Toolik Inlet	500	Plane bed	Cobble	3	0.64
P1	ISwamp-Inlet	250	Beaded	Peat	2	0.90
AP	Oksrukuyik	275	Beaded	Gravel and Peat	3	0.16

[a]The reach locations are noted in Figure 1, and stream names refer to the nomenclature designated by the Arctic LTER site.

streams has been described previously by *Peterson et al.* [1993], *Edwardson et al.* [2003], and the references therein.

3. Methods

3.1. Tracer Experiments

[12] Multiple stream tracer experiments were conducted at each of the five geomorphically distinct stream reaches on different days throughout the thaw season to compare responses to dynamic flow and active layer thaw conditions. Each tracer test consisted of a slug of Rhodamine WT (RWT) injected at a location that promoted complete vertical and horizontal mixing across the stream. The appropriate slug injection mass was determined by standard mixing calculations [*Fisher et al.*, 1979]. At the end of each reach, for all experiments, in situ stream RWT concentrations were measured continuously with a Turner Designs 10-AU fluorometer (Turner Designs, Incorporated, Sunnyvale, California) fitted with a flow-through cell, temperature compensation and data acquisition system. The injection and downstream sampling points were the same for all experimental reaches throughout the repeated tracer experiments.

[13] Rhodamine WT is not a completely conservative tracer, as it is known to sorb to streambed material [*Bencala et al.*, 1983]. Recently, R. Haggerty (personal communication, 2006) has found that sorption and desorption occurred in a column RWT experiment using <2 mm size fraction of streambed sediments. We did not take into account sorption-desorption processes in our simulations. In our repeated experiments, we expected that any sorption would be minor and similar from experiment to experiment within the same reach.

3.2. Solute Transport Simulation

[14] Transport models based upon a single mass transfer coefficient do not always adequately simulate the observed distribution of stream tracer concentrations over time at downstream monitoring stations (breakthrough curves (BTCs)) during late times of solute injection experiments [e.g., *Gooseff et al.*, 2003]. However, *Haggerty and Reeves* [2002] and *Haggerty et al.* [2002] describe a 1-D solute transport model (STAMMT-L) that uses a general distribution of residence times rather than a single fixed residence time and has greater success in simulating late time BTC observations. We used this model to provide optimized parameters for reach-representative estimates of advection, dispersion, and transient storage for each of our solute addition experiments. These values, and metrics derived from them, were then compared across the thaw season and morphologies.

[15] The STAMMT-L model applies a user-specified residence time distribution (RTD) to the general one-dimensional advection-dispersion transport equation. The transport equation for a system that is initially tracer-free with no longitudinal inputs is

$$\frac{\partial C}{\partial t} = -u\frac{\partial C}{\partial x} + D\frac{\partial^2 C}{\partial x^2} - \beta_{tot}\frac{\partial}{\partial t}\int_0^t C(\tau)g^*(t-\tau)d\tau \quad (1)$$

where u is the mean in-stream advection velocity (m s^{-1}), D is the longitudinal dispersion (m^2 s^{-1}), β_{tot} is the ratio of

the mass in the immobile zone to that in the mobile zone at equilibrium, C is the solute concentration in the stream (μg L^{-1}), and τ is a lag time (s). In the last term of equation (1), $g^*(t)$ is convolved with the stream concentration to represent exchange with the transient storage zone following an appropriate RTD. The probability density function that the solutes remain in storage after a time, t, is defined as

$$g^*(t) = \sigma e^{-\sigma t} \quad (2)$$

for an exponential RTD where σ is the first-order rate coefficient (s^{-1}). This is similar to the standard first-order model provided by *Bencala and Walters* [1983] and implemented numerically by *Runkel* [1998] in the U.S. Geological Survey OTIS model. The OTIS model has a storage exchange rate α (referred to herein as α_{OTIS}) that is equivalent to the product of σ and β_{tot}, where β_{tot} is equivalent to the ratio of storage area (A_s) to stream cross-sectional area (A). The $g^*(t)$ for a power law RTD in the storage zone is expressed as

$$g^*(t) = \frac{(k-2)}{(\sigma_{max}^{k-2} - \sigma_{min}^{k-2})}\int_{\sigma_{min}}^{\sigma_{max}} \sigma^{k-2}e^{-\sigma t}d\sigma \quad (3)$$

where k is the power law exponent, which corresponds to the slope of late time concentration tail after a pulse injection [*Haggerty et al.*, 2002]. Equation (3) defines a power law function bounded by σ_{max} and σ_{min}, with behavior $g^*(t) \sim t^{1-k}$ between the inverse of those limits. These limits are determined by bracketing the timescales of the BTC from the tracer experiment; σ_{max} was always chosen to be 10^{-1} s^{-1}, and σ_{min} was always chosen to be the last time of data acquisition in the field, since the injection.

[16] Parameters were estimated within STAMMT-L using a nonlinear least squares algorithm [*Marquardt*, 1963] that minimized the sum of square errors on the logarithms of concentrations. For all simulations, we report root mean squared error (RMSE) as defined by *Bard* [1974, p. 178], in which a value of 0 indicates a perfect fit of the simulated values to the observations. Optimization runs for all tracer tests were completed using both RTD methods and the one that generated the lowest RMSE was accepted as the best model. Depending on the RTD type, parameters u, D, β_{tot}, k, and σ were optimized.

3.3. Metrics Characterizing Transient Storage

[17] Two metrics were computed with the optimized transport model parameters to further characterize solute storage in the study reaches. First, mean storage residence time, t_{stor} (s), which represents the average time interval that a water particle spends within a storage zone, was computed as $1/\sigma$ for exponential RTD simulations and as the inverse of the harmonic mean of σ_{min} and σ_{max} for power law RTD simulations. The second metric was hydrologic retention, R_h (s m^{-1}) [*Morrice et al.*, 1997], which represents both the amount of time a water particle spends in storage and the average distance it travels in the channel before entering into a storage zone. Hydraulic retention is a good metric to compare among reaches, because it describes the effects of

storage on in-stream solute transport. In the case of our analysis, it was computed as

$$R_h = \frac{\beta_{tot}}{u} \quad (4)$$

which is equivalent to the following version put forth by *Harvey et al.* [2003], $R_h = A_s/Q$, where A_s is the modeled reach-average storage zone cross-sectional area.

[18] In an effort to characterize hydraulic conditions that could be used for comparison to transient storage metrics, we computed two descriptors of the hydraulics within the stream at the time of the tracer experiments. The first of these is the Darcy-Weisbach friction factor (f), which has been associated with transient storage characteristics in other studies [*Legrand-Marcq and Laudelout*, 1985; *Harvey and Wagner*, 2000; *Harvey et al.*, 2003]. It was calculated as

$$f = \frac{8gdS}{u^2} \quad (5)$$

where g is the gravitational constant, d is reach-average stream depth (m), and S is the slope of the energy grade line for uniform flow over the reach and does not account for smaller-scale variations. The value for S was estimated from the channel slopes, which were determined from detailed topographic streambed and water surface surveys. Reach-average stream depth was estimated as A/w. The cross-sectional area of the surface flow, A, was calculated as the quotient of Q and u, while w represents the mean channel width measurements collected in the field at the time of the injection.

[19] The second term used to characterize channel hydraulics is stream power per unit of bed width, ω (N m^{-1} s^{-1}). Unit stream power was computed for each reach at the time of the solute injection, as

$$\omega = \frac{\Omega}{w} = \frac{\gamma SQ}{w} \quad (6)$$

where, Ω is total stream power (N s^{-1}) and γ is the specific weight of water (N m^{-3}) [*Dingman*, 1984]. Unit stream power represents the downstream energy flux over the streambed per unit time, and therefore can be compared through time at each reach and across reaches despite differences in channel morphology and discharge.

3.4. Monitoring Depth of Thaw

[20] Ground-penetrating radar (GPR) and in situ thermistor profiles were used to monitor the depth of thaw in and adjacent to the streambed. Following the methods given by *Brosten et al.* [2006], we collected GPR and thermistor profiles at cross sections within 3 of the 5 study reaches (A1, A2, and P1) and only GPR data at the other two sites (A3 and AP). Data from the thaw depth monitoring were used in conjunction with the hydraulic modeling to corroborate and expand our hydraulic interpretations of how transient storage shifts relate to changes in hyporheic extent through the thaw season. The use of GPR to observe subsurface thaw conditions has been demonstrated in previous studies [e.g., *Bradford et al.*, 2005].

4. Results

4.1. Tracer Experiment Simulations

[21] The BTCs and simulations from A1 (1 June 2004) and P1 (2 June 2004) are representative of the goodness of

model fit for all tests as well as the time series completeness in the BTCs (Figure 2). Figure 2 also demonstrates key differences in BTCs observed between sites and dates. The BTC for site A1 is characteristic of an advection-dominated pulse while the BTC for site P1 is characteristic of pulse transport more influenced by dispersion. Figure 2 also illustrates the importance of applying the optimal RTD to a solute transport simulation. For example, the simulation for the experiment run at site P1 on 2 June 2004 has a RMSE of 0.30 for a power law RTD (Figure 2d), whereas the application of an exponential RTD created a better optimization with an RMSE of 0.12 (Figure 2c). Of the 12 tracer tests conducted in alluvial reaches, 9 were best simulated with power law RTDs. The 3 experiments which had exponential RTDs occurred in A2 during the three earliest and lowest-flow conditions observed in this reach (Table 2). All of the optimal simulations in the peat reaches (P1 and AP) were best fit with exponential RTDs. The separation between power law and exponential RTDs models was generally observed in the advective velocity, where the experiments with relatively high advective velocities (>0.15 m s^{-1}) were best explained by power law RTDs while experiments with slow advective velocities (<0.15 m s^{-1}) were best explained by exponential RTDs.

4.2. Depth of Active Layer Thaw and Stream Discharge Regimes

[22] In each reach, the initial observation of average thaw depth was unique (Figure 3). Thaw depth advanced rapidly early in the summer season across all sites, but became asymptotic or retreated by middle to late summer. The greatest thaw depth was found in the alluvial reach, A1, with a mean depth of 2.03 m on 6 August 2004. The least thaw occurred below P1, a peat reach with little to no alluvium. It should be noted that the thaw had initiated in all sites prior to the first GPR profile collection.

[23] Stream stage data at A3 (Figure 4a) are representative of the regional stream hydrograph characteristics during the summer thaw season of 2004. Each of the study reaches experienced discharge recession, similar to A3, during the months of June and July (Table 2). However, four region-spanning rain events during the months of July and August created elevated flow events under which the late season tracer tests were conducted.

4.3. Transient Storage Dynamics

[24] For all reaches, β_{tot} and t_{stor} values were generally higher in June and lower in August, but neither parameter was well correlated with the extent of thaw (Figure 4). Values for β_{tot} were all greatest during the first half of the thaw season, with A3 demonstrating the greatest value at 1.63 on 9 June 2004 (Figure 4a). Values for β_{tot} declined substantially in all reaches by late in the thaw season with A3 decreasing to 0.12 by 5 August 2004. Similarly, t_{stor} was greatest and most varied across reaches during the early thaw season, but eventually decreased during August (Figure 4c). Values for β_{tot} and t_{stor} did not always correlate with thaw depths (Figures 4b and 4d). For example, the values for t_{stor} in the A3 reach increased linearly with greater thaw depths, as the active layer thickness grew from 0.6 to 1.1 m. However, on the same reach, t_{stor} decreased 31-fold during a later experiment when thaw depth was still near 1.0 m.
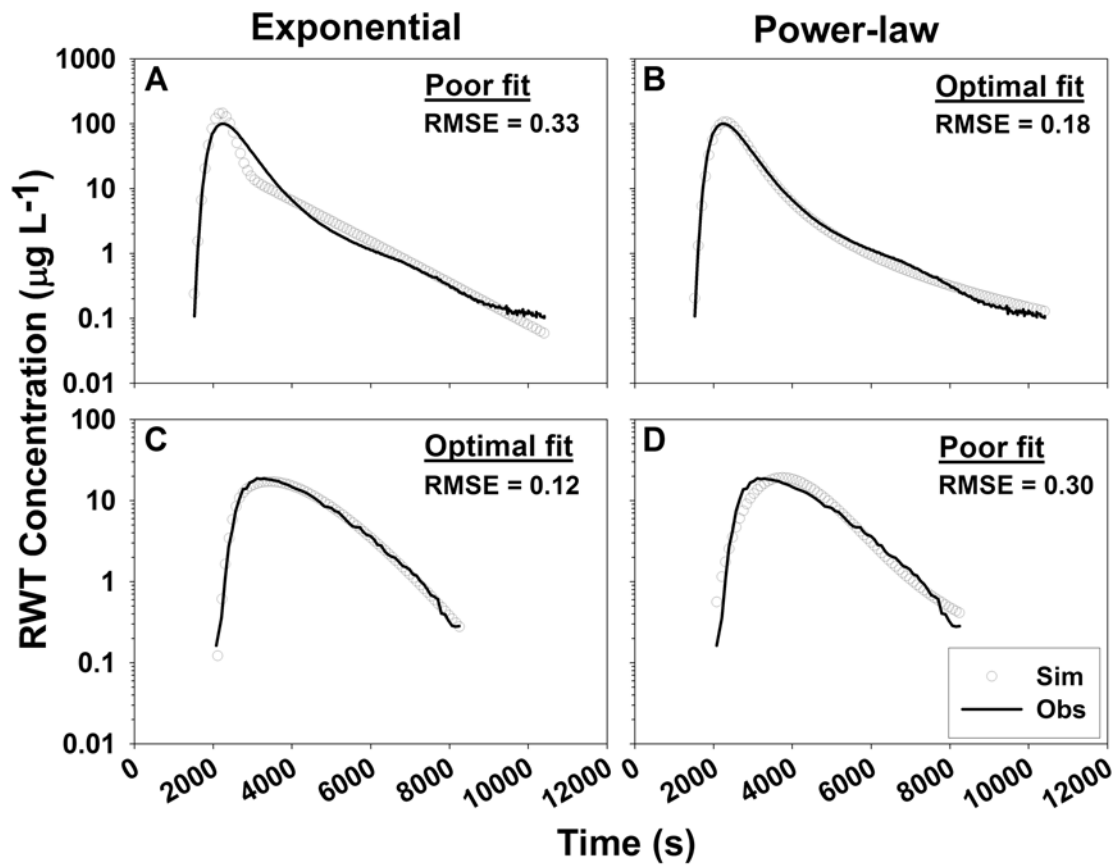
Figure 2. Representative exponential and power law residence time distribution (RTD) simulations for alluvial reach A1, 1 June 2004, tracer experiment (a and b), and peat reach P1, 2 June 2004, experiment (c and d) Rhodamine WT breakthrough curves.

Table 2. Discharge Conditions, Optimized Solute Transport Model Parameters, Transient Storage Metrics, and Transport Model Goodness of Fit Statistics for All Stream Tracer Experiments[a]

Stream	Date	Q, m^3 s^{-1}	u, m s^{-1}	RTD	RMSE	β_{tot}	D, m^2 s^{-1}	α, s^{-1}	k	t_{stor}, s
A1	6/1/04	0.25	0.25	Power law	0.18	0.17	1.96	0.0013	2.23	787
	6/24/04	0.05	0.12	Power law	0.23	0.39	2.05	0.0005	2.18	2096
	8/7/04	0.43	0.50	Power law	0.16	0.18	1.11	0.0031	2.33	322
	8/18/04	0.34	0.48	Power law	0.17	0.31	1.33	0.0032	2.5	309
A2	6/3/04	0.31	0.19	Exponential	0.14	0.26	1.51	0.0018	...	202
	6/9/04	0.12	0.09	Exponential	0.12	0.29	1.09	0.0009	...	323
	6/18/04	0.09	0.07	Exponential	0.20	0.25	1.71	0.0005	...	549
	8/6/04	0.82	0.69	Power law	0.21	0.05	1.22	0.0048	2.11	208
A3	6/4/04	0.59	0.29	Power law	0.19	1.02	1.41	0.0005	1.75	2045
	6/9/04	0.35	0.20	Power law	0.22	1.63	1.56	0.0003	1.78	2976
	6/17/04	0.26	0.16	Power law	0.18	1.11	1.48	0.0002	1.71	4464
	8/5/04	2.04	0.77	Power law	0.21	0.12	0.38	0.0070	2.5	143
P1	6/2/04	0.28	0.09	Exponential	0.12	0.55	1.59	0.0024	...	234
	6/25/04	0.05	0.02	Exponential	0.12	0.76	1.75	0.0003	...	2836
	8/6/04	0.46	0.16	Exponential	0.25	0.23	2.63	0.0026	...	118
	8/16/04	0.26	0.13	Exponential	0.18	0.38	1.31	0.0018	...	213
AP	6/5/04	1.31	0.20	Exponential	0.25	0.50	1.73	0.0018	...	283
	6/12/04	0.58	0.12	Exponential	0.27	0.78	1.81	0.0008	...	957
	6/21/04	0.44	0.09	Exponential	0.26	0.55	1.94	0.0006	...	972
	8/5/04	2.70	0.52	Exponential	0.28	0.53	2.86	0.0042	...	127

[a]Note that the reported α values are either the α_{OTIS} for exponential simulations or the harmonic mean of the applied σ values for power law simulations. RTD is residence time distribution.
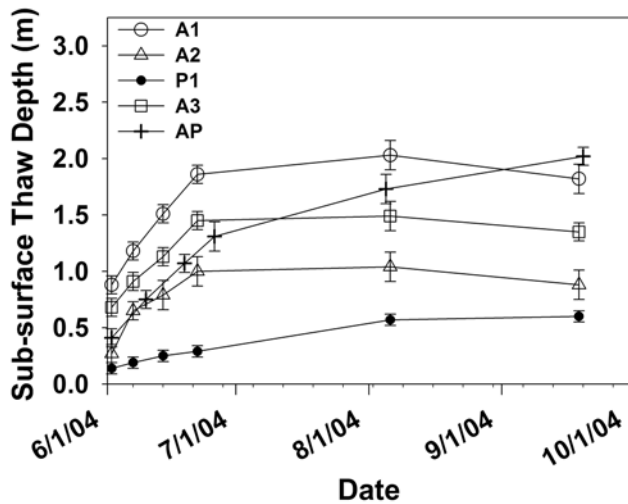
Figure 3. Characterization of single cross-sectional mean active layer depth through the thaw season for each reach. Note that alluvial reaches (A1, A2, and A3) have open symbols, while the peat (P1) and alluvial peat (AP) reaches are represented by closed circles and crosshairs, respectively. Error bars represent the resolution error associated with each ground-penetrating radar measurement.

[25] The greatest values of β_{tot} and t_{stor} modeled for each reach generally occurred during periods of low-flow conditions in the region; much lower values were observed during the higher-flow period in August. Mean storage residence time exponentially decayed with increasing discharges at each reach (Figure 5a). The greatest range in t_{stor} with discharge occurred in A3, where it varied from 143 to 4,464 s. Discharge was strongly related to t_{stor} at each site, explaining between 72% and 99% of the variation at A2 and AP, respectively. The β_{tot} values showed similar patterns, albeit somewhat weaker at some sites (R^2 = 0.22 to 0.91 at AP and A2, respectively), with linear decreases as flow increased (Figure 5b). The general relationships between discharge and both t_{stor} and β_{tot} are consistent; however, the specific relationships between these variables differ among the different geomorphological reaches studied here.

[26] The relationship between u and Q values at each reach was robust, but the rate of change between the two variables varied across sites (Figure 6a). The u:Q relationships can be partitioned by reach morphologies, where the most rapid changes in advective velocity in response to increasing discharge was seen in the two alluvial pool-riffle reaches. On the other hand, the reaches with the least change in u in response to discharge were the two peat reaches. The A3 site with its broad, plane bed morphology had intermediate rates of change between u and Q. Figure 6b
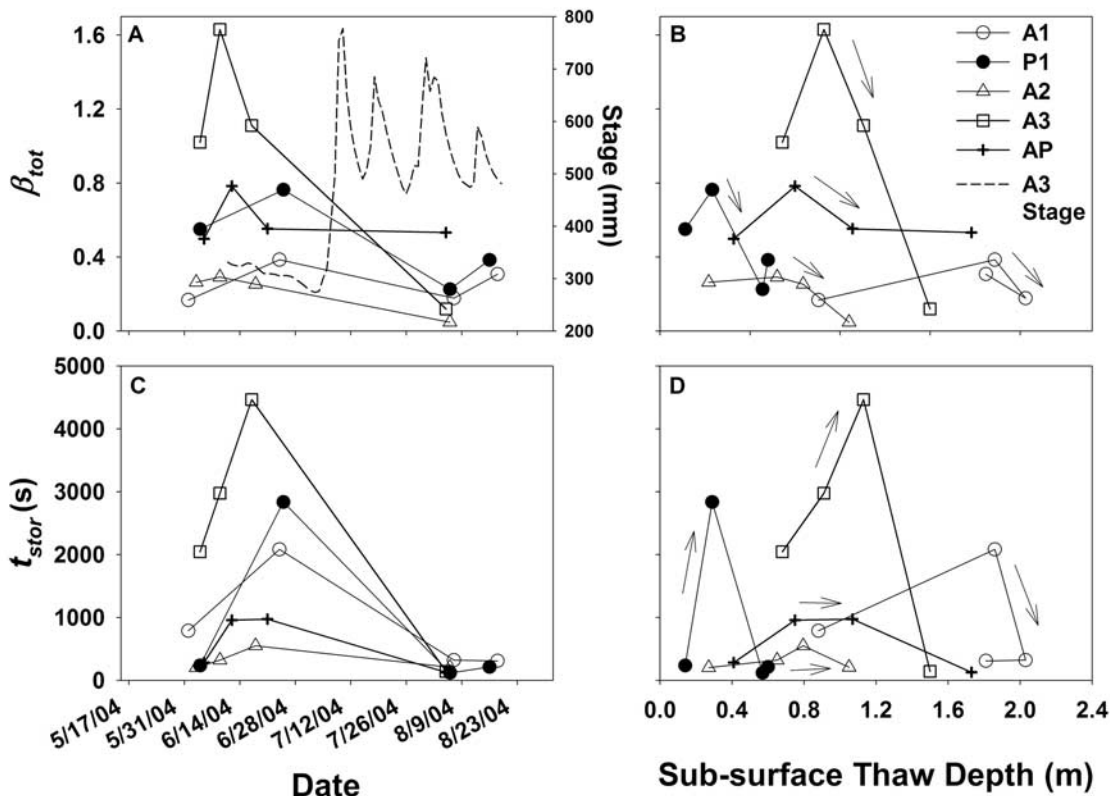
Figure 4. Relationship between reach-average transient storage metric, β_{tot}, and (a) time and (b) depth of thaw. Relationship between reach-average transient storage metric, t_{stor}, and (c) time and (d) depth of thaw. Note each series in Figures 4b and 4d is sequential through time as indicated by the arrows and may demonstrate hysteresis in relationships. The discharge dynamics for the study region are demonstrated by A3 stage variance in Figure 4a (dashed line).
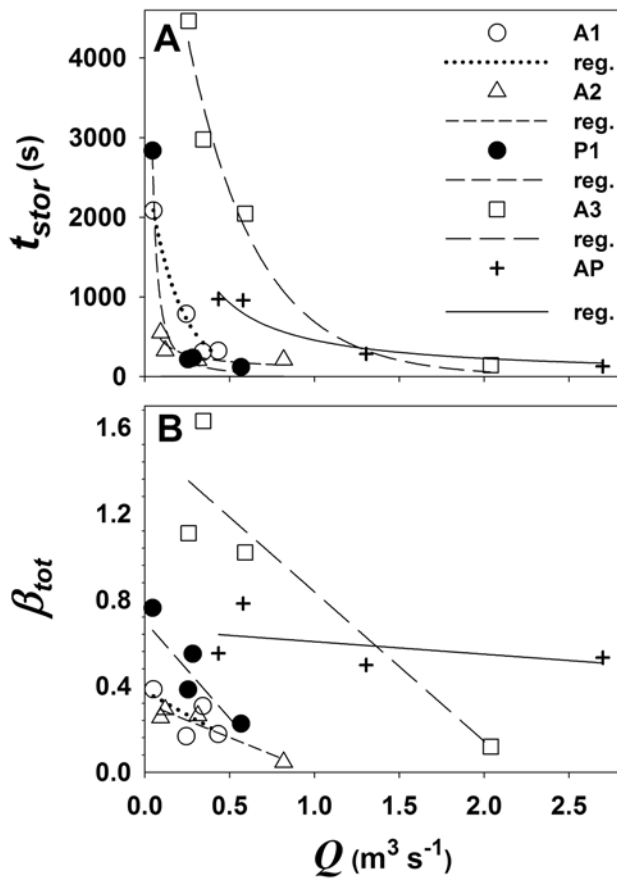
Figure 5. The relationship between discharge and (a) t_{stor} and (b) β_{tot} for each reach.

shows the values of α_{OTIS} in reaches A2, P1, and AP linearly increased with Q. The values for α_{OTIS} are only available from exponential RTD simulations and cannot be generated for the power law RTD optimizations because the solution applies a range of exchange rates. The k values from the power law simulations (i.e., A1 and A3 tracer experiments) also demonstrated linear increases with Q (Table 2).

[27] In our analysis of the Darcy-Weisbach friction factor, we found that f exponentially decreased with increasing Q, which is to be expected, given that a Q imposes localized u and f properties. All f values were well within the range observed in temperate streams [*Harvey and Wagner*, 2000, Figure 12]. Friction factor was directly related to t_{stor}, and indirectly related to α_{OTIS} (Figure 7). Thus the greatest t_{stor} and smallest α_{OTIS} values were observed during discharges where there is a large amount of flow resistance (i.e., low-flow conditions).

[28] As was the case with comparisons to Q, t_{stor} declined exponentially with increasing ω for all reaches (Figure 8a). However, the apparent differences in morphologies and flow regimes that separate the streams in Figure 5a (the comparisons with f) generally diminished when comparing different stream powers. Furthermore, we found a simple linear relationship between ω and values of α_{OTIS} (Figure 8b, $R^2 = 0.76$) despite major differences in reach morphology (i.e., beaded peat to alluvial step-pool) and flow regimes ($0.05-2.7$ m^3 s^1).

[29] To generalize transient storage comparisons across all of the reaches, between the two main morphologic groups of peat and alluvial channels, and for comparison to the hydraulic metrics (f and ω), we calculated hydraulic retention, R_h, values for each experiment (Figure 9). Across all reaches S and Q were poorly correlated with hydraulic retention (R_h), with R^2 values of 0.05 and 0.29, respectively (Figure 9a). Both f and ω_A were more strongly correlated to R_h with R^2 values of 0.48 and 0.57, respectively.

5. Discussion

[30] In this investigation, we compared analyses of transient storage in a wide variety of streams and related these analyses to different hydraulic, morphologic, and permafrost conditions in the streams. Previous stream tracer investigations, especially in the Arctic, have been limited to taking a "snapshot" approach, where interpretations can be confounded by temporal variability in hydrology and morphology [e.g., *Edwardson et al.*, 2003]. Other studies, such as *Harvey et al.* [2003], have made advances from repeated transient storage assessments in streams, conducted across different discharges and even shifts in surface channel morphology. However, it is simpler to interpret the influence of Q and morphology on transient storage in the Arctic headwater streams of this study because they lack larger exchange processes associated with deep groundwater
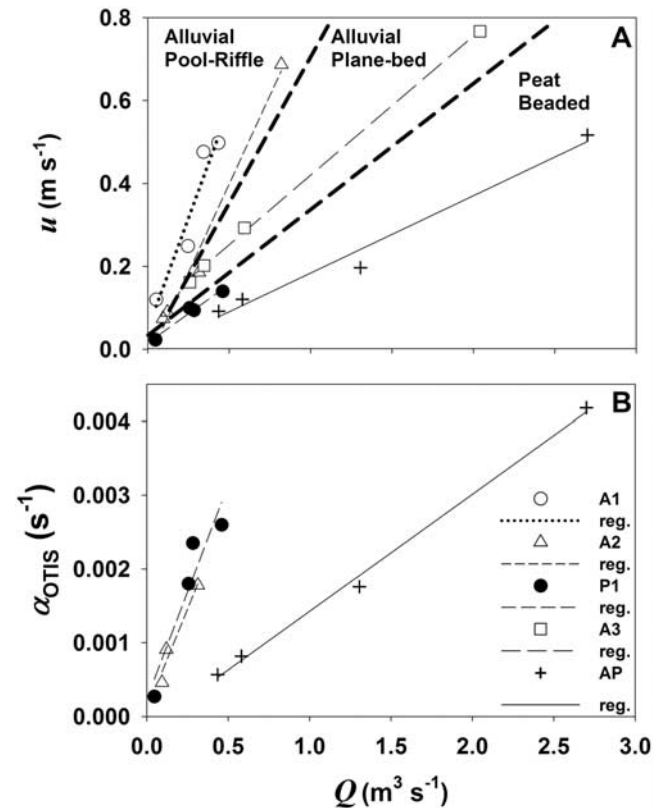
Figure 6. For each reach: relationship between u (a), α_{OTIS} (b), and discharge. Note: α_{OTIS} values could only be generated for the three reaches (A2, P1, and AP) that applied exponential RTD in the simulation model. Thick dashed lines in Figure 6a represent potential morphologically based u:Q slope domain boundaries.
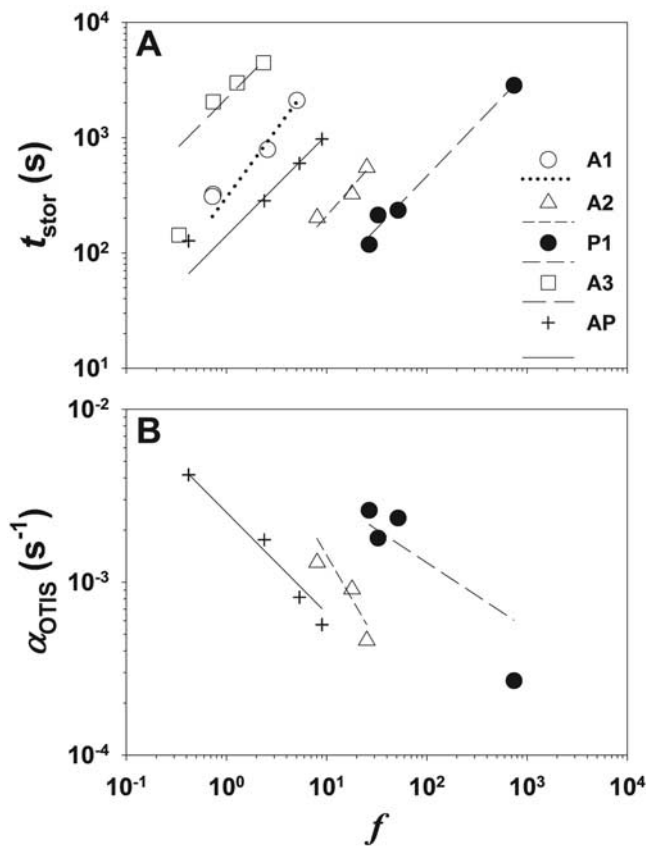
Figure 7. For each reach, relationship between t_{stor} (a), α_{OTIS} (b), and f. Note: α_{OTIS} values could only be generated for the three reaches (A2, P1, and AP) that applied exponential RTDs in the simulation model.

aquifers and sediments lateral to the active channel. These stream channels are effectively bound by permafrost, so groundwater–surface water exchange is limited and consequently constrained by the depth of thaw below the channel.

5.1. Differences Between Expected and Observed Transient Storage Dynamics

[31] The results of the tracer experiments and subsequent modeling do not directly support our expectations that hyporheic zone size and its influence on transient storage increases with depth of thaw below the channel. Neither β_{tot} nor t_{stor} were consistently related to the size of the thaw bulbs. However, during the low-flow portion of the season, there does appear to be some relationship between active layer thaw depth and transient storage. This relationship disappears or becomes undetectable under high discharge conditions. Therefore because of the hydrologic variability, it is not possible to definitively partition whether in-channel or active layer thaw dynamics drive the observed transient storage conditions. However, a comparison of hydrologic conditions across the tracer tests completed during the 2004 thaw season suggests that both in-channel and hyporheic storage influence the transient storage results and that their respective influence will vary primarily with Q and to a much lesser extent with increasing thaw depth. Future studies should be focused on direct observations of the hyporheic sediment and exchange properties (e.g., hydraulic

conductivity and vertical head gradients), which might help to partition the hyporheic influence on transient storage.

5.2. Discharge Relations to Transient Storage Metrics

[32] To better explain the observed dominance of discharge on transient storage conditions, we explored discharge-related metrics and their relationship to modeled storage parameters. The behavior of β_{tot} across the various reaches we studied indicated that all reach-representative storage zones were sensitive to discharge. However, some were more sensitive than others as indicated by the different rates of change seen in Figure 5. Contrary to *D'Angelo et al.* [1993], the largest streams in this investigation possessed the highest β_{tot} values. The decline in β_{tot} values with increasing Q in each reach suggests that the dominant storage zones present at lower discharges were assimilated into the main flow path under higher-flow conditions. Mean storage residence time reflects similar behavior and likely shares the same explanation. However, in relation to Q, β_{tot} decreased in a linear fashion, whereas t_{stor} declined exponentially. This t_{stor} relationship indicates that the surface storage features may be exponentially sensitive to different stage conditions in the reaches. Furthermore, as expected from hydrodynamic theory and the direct relationship between velocity and hyporheic exchange [*Packman and Salehin*, 2003], the rate of exchange (α_{OTIS}) between the main flow and the storage zones increased with discharge and velocity across all experiments best fit by exponential
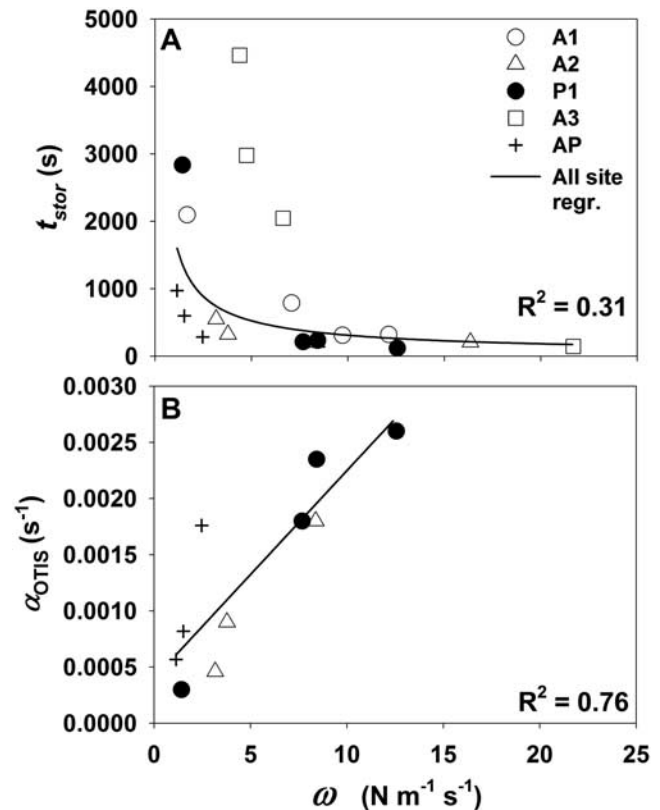
Figure 8. Relationship between (a) t_{stor}, (b) transient storage exchange rate, α_{OTIS}, and unit stream power, ω, for all tracer addition experiments. Note that α_{OTIS} values could only be generated for the three reaches (A2, P1, and AP) that applied exponential RTDs in the simulation model.
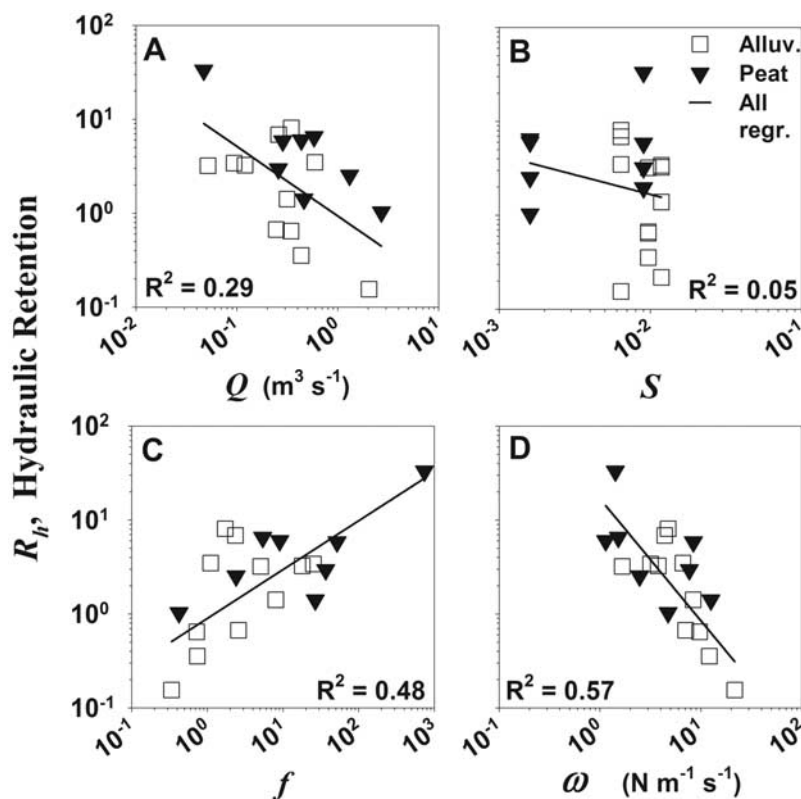
Figure 9. For all tracer addition experiments: relationship between (a) Q, (b) S, (c) f, and (d) ω, and hydraulic retention. Note that sites were simplified to either alluvial- or peat-influenced reaches (open squares and closed triangles, respectively).

RTDs (Figure 6b). This result is consistent with field and flume investigations (*D'Angelo et al.* [1993] and *Elliott and Brooks* [1997], respectively) and is likely due to increased advection and turbulent flow rates (i.e., flushing) within storage zones.

5.3. Morphologic Relations to Transient Storage

[33] If transient storage in these systems is dominated by discharge and associated velocities, then morphology must also play a role, because the relationship between Q and u is different in every reach and is dictated by morphologic impacts on hydraulics. For example, the observed relationship between Q and u is similar between the two alluvial reaches, as are the relationships between β_{tot} and t_{stor} and Q in these reaches. Thus morphology does influence the sensitivity of a reach to changes in surface flow hydraulics which in turn likely affects in-channel storage zones. The morphology of P1 (i.e., shallow gradient and incised peat channel with a very small width to depth ratio) creates a stream with a large surface water volume, relative to total discharge. This stream also exhibits large rates of change in β_{tot} when discharge changes. This β_{tot} characteristic of P1 is likely due to in-channel storage changes with discharge, because the morphology does not permit extensive influence from a hyporheic storage zone (i.e., max thaw depth was less than 0.6 m). Instead, the P1 morphology promotes low-flow surface dead zones (e.g., pool margins or eddies), which are easily incorporated into the main flow under higher discharges. *Edwardson et al.* [2003] also reported that surface storage zones can dominate transient storage in

Arctic streams. Furthermore, the highest β_{tot} values found during low-flow conditions were always found at the plane bed A3 site, where surface flow was rarely located within a thalweg; rather it was spread across the entire channel width creating many tortuous surface flow paths and an extensive boundary surface area relative to stream flow. At high flows, the value of β_{tot} at A3 dropped by an order of magnitude. This is likely due to a more uniform surface flow found during higher stages which inundates the substrate decreasing the boundary surface area. This inundation influence on transient storage is similar to the concepts regarding bed form amplitude and flow conditions put forth by *Packman and Bencala* [2000] and observed by *Zaramella et al.* [2003].

[34] Early season indicators of transient storage (t_{stor} and β_{tot}) observed in A3 could also be explained if the hyporheic zone in this reach was more extensive than at the other reaches. This reach had the largest width to depth ratio of all of the reaches sampled in this study, with relatively shallow surface flow occurring across the majority of the channel, and significant depths of thaw below the channel. The combination of these conditions may have promoted a relatively large hyporheic storage zone as indicated by values of β_{tot} and t_{stor} observed during the early season. However, even under this scenario, large discharges in A3 overwhelmed the potential storage influence of a well developed hyporheic zone during the late summer experiments. These observations are similar to the findings of *Elliott and Brooks* [1997] who demonstrated in flume studies, that the effect of hyporheic exchange on surface

flow processes decreased with increased discharge. Furthermore, in their experiments, flow depth and corresponding cross-sectional area of the stream often increased without increases in bed area.

5.4. Combined Influence of Discharge and Morphology on Transient Storage

[35] The relationship between t_{stor} and Q clearly indicates that the residence times observed in these study reaches were highly sensitive to discharge. Furthermore, the observed relationships between u and Q at these sites illustrate that morphology imparts a significant influence on the response of velocity to changes in discharge. Therefore given the sensitivity of transient storage to advective velocity in the modeling process, the generated transient storage conditions also reflect the morphologic differences within the reaches. Logically, other hydraulic characteristics of the study reaches, such as the rate of exchange between storage and transport flow (α_{OTIS}) and the Darcy-Weisbach friction factor (f), also vary with discharge because they are either directly or indirectly influenced by the components that affect discharge.

[36] To explore the combined influence of discharge and morphology, reach-descriptive metrics that integrate the two components were calculated and compared to transient storage metrics. The Darcy-Weisbach friction factor was used previously to relate stream conditions to transient storage dynamics [Bencala and Walters, 1983; Legrand-Marcq and Laudout, 1985; Harvey and Wagner, 2000; Harvey et al. 2003]. Consistent with these earlier studies, we found that f was negatively related to Q. This relationship is likely consistent because of the sensitivity of f to changes in the squared velocity term present in the denominator (equation (6)). More fundamentally, f is controlled by the relative roughness (i.e., boundary roughness relative to flow depth), which generally decreases as larger discharges increase flow depths that in turn reduce relative roughness. Both cases result in larger f values normally associating with smaller discharges. Therefore f values should be positively related to transient storage, which was the case in this study with the greatest t_{stor} values occurring at low flows. Harvey and Wagner [2000] and Harvey et al. [2003] illustrate that this dimensionless metric can be used as a prediction for transient storage behavior in a stream without the use of more complicated techniques, such as transport modeling. In this investigation, f also correlates well with the observed transient storage conditions and serves to collapse the results of the various sites onto one trajectory when comparing to R_h. However, changes in f did not successfully explain the variability in t_{stor} and α_{OTIS} values observed across the reaches.

[37] In the case of our study, t_{stor} was found to clearly covary with stream power per unit bed area, as expected, on the basis of the earlier established relationship between t_{stor} and Q. Each stream displayed a similar trend in decreasing t_{stor} with increasing ω_A (and Q), however assessment of ω tended to collapse the range of variability among all reaches. The ability of ω to normalize the hydrologic and morphologic variability among sites is apparent in comparison to α_{OTIS} values. The correlation between ω and transient storage descriptors, t_{stor} and α_{OTIS}, appears more robust across all sites in comparison to Q. This makes sense because ω incorporates Q and basic morphologic descrip-

tion of the system (S and w), and these in turn ultimately set the template for transient storage conditions.

[38] To explore the possibility of using ω as a predictive and explanatory metric for transient storage, we conducted a simple comparison of hydraulic retention with Q, f, and ω. This analysis demonstrated that R_h was most strongly correlated with ω. Moreover, a predictive model of transient storage, such as the one put forth by Harvey et al. [2003] would be more robust by including ω. Coupling this metric with additional knowledge about geomorphic controls on surface (e.g., sub-reach-scale slope variability) and hyporheic flow conditions may lead to more accurate characterizations of overall stream storage potential, where it occurs, and ultimately, where there may be ''hot spots'' for transient storage and the ecological dynamics associated with transient storage.

[39] Both ω and f (or equivalents metrics) are already used in river restoration design because of their importance in achieving desired stream hydraulic and sediment transport conditions. However, the intrinsic link between these physical conditions of a stream and its ecological characteristics (e.g., biogeochemistry) points to ω and f as potentially useful tools for future river restoration efforts where adding ecological value is also a goal. For example, ω is a hydraulic condition that can be designed for if the prevailing discharge conditions and stream slopes are considered. Therefore if increasing transient storage potential and the range of water residence time distributions within a restored reach is a goal, designers can incorporate ω and f into their restoration process to assist in determining or predicting postrestoration transient storage dynamics. This is encouraging in light of the increasing acknowledgment that transient storage within streams, especially as it relates to hyporheic processes, is as an often overlooked, but important consideration for river restoration [e.g., Vervier et al., 1993; Collier et al., 2004; Wohl et al., 2005].

5.5. Transient Storage Dynamics in Arctic and Temperate Streams

[40] The results from this investigation indicate that these Arctic tundra streams during the thaw season behave similarly to equivalently sized temperate streams in terms of transient storage dynamics. Work from temperate stream investigations [Legrand-Marcq and Laudelout, 1985; D'Angelo et al., 1993; Harvey et al., 2003] report mean β_{tot} values that range from 0.2 for a small forested stream up to 0.6 for a semiarid alluvial stream. The average β_{tot} value for our reaches with similar discharges (i.e., A1, A2, and P1) was 0.31, which is remarkably similar to the findings of Edwardson et al. [2003] who reported a mean β_{tot} value of 0.32 for comparable Arctic streams.

5.6. Uncertainty Associated With Transient Storage Modeling

[41] The transient storage modeling results of this investigation are in general agreement with other similar studies [e.g., D'Angelo et al., 1993; Edwardson et al., 2003; Harvey et al., 2003]. The modeled parameters and how they relate to reach conditions are similar to these earlier studies. However, Harvey and Wagner [2000] and Wondzell [2006] point out that while modeled parameters can appear to be acceptable, they can be at odds with observations of the hyporheic transient storage (i.e., samples from hypo-

rheic zone wells). For example, *Wondzell* [2006] found that while model results indicated dramatic shifts in storage conditions under high- and low-flow conditions, there was little to no change in the hyporheic dynamics. This observation can be explained by assuming that Q dominates surface storage zones, which results in shifts of modeled transient storage. However, another explanation is that of the "window of detection" [*Harvey and Wagner*, 2000]. The "window of detection" represents the range of transient storage and residence times that any particular tracer test is sensitive to given the process timescales created from flow velocity, the duration of the tracer test, and reach lengths. Therefore the results of the transient storage modeling in this investigation may reflect the sensitivity of our methods to certain ranges of flow and reach lengths. For example, across the range of hydrologic conditions of the present investigation, u appears to generally predict the best RTD (i.e., exponential or power law) to apply for each tracer test. Subsequently, the applied RTD constrains the output of transient storage parameters. Thus the transient storage conditions generated for these streams may be particularly sensitive to flow conditions.

[42] Unfortunately, there are insufficient techniques available to determine if the modeling represents the true transient storage characteristics or if they are artifacts of the applied tracer and modeling method limitations. Consequently, future work should include (1) more frequent and longer (constant rate) tracer additions experiments, (2) inclusion of hyporheic sediment and exchange sampling through the use of well arrays, (3) more frequent and spatially explicit GPR thaw imaging of the channel to better characterize thaw conditions on scales larger than a single cross section, and (4) develop groundwater surface flow models that will integrate transport observations in both the surface and subsurface flow paths.

6. Conclusions

[43] Results from this investigation demonstrated that selected transient storage model parameters t_{stor}, β_{tot}, and α_{OTIS} reflect differences in Arctic stream characteristics such as discharge and morphological conditions. These model parameters were useful descriptors across a diversity of stream types. Given the simplicity of these systems (i.e., generally fixed morphology and very limited potential for groundwater aquifer–surface water exchange) and their variable flow conditions, a comparison of streams transient storage response to various physical conditions was feasible at the reach scale.

[44] The observed relationship between transient storage and discharge emphasizes the main thrust of this investigation, which was to shed light on how transient storage dynamics relate to shifts in the physical conditions (i.e., discharge, morphology, and active layer thaw) of a stream. In particular, we found that transient storage is strongly correlated with the hydraulic metric of unit stream power. We also found good correlations between discharge and Darcy-Weisbach friction factor and several metrics of transient storage. Unit stream power is a relatively simple metric to calculate and may provide important insight into stream transient storage characteristics, such as relative changes in t_{stor}, α_{OTIS}, and R_h. The success of stream power as a predictor of stream transient storage characteristics lies

in its ability to normalize simple characteristics of discharge and morphology, thereby allowing better comparisons to be made across streams with different scales of flow and morphology. This suggests a possible direction for the integration of additional independent variables into future physically based models for solute transport and storage in streams. Moreover, f and ω may serve as tools for river restoration designers because they provide a quantifiable link between transient storage and stream morphology and require minimal field reconnaissance or data acquisition (e.g., ω only requires knowledge of stream slope, width, and discharge). Furthermore, the strength of the relationship between reach-average transient storage metrics and discharge is encouraging in itself because it reinforces the notion that despite the existence of great heterogeneity and complexity through time and space within stream systems, there are driving mechanisms that are dominant to the extent that this complexity becomes inconsequential at the reach scale. Future work will need to determine the appropriate ranges of transient storage sensitivity to Q. This will allow physically based models to possibly avoid inaccurate simulations of transient storage dynamics by constraining the range of solutions for given hydrologic conditions.

References

Bard, Y. (1974), *Nonlinear Parameter Estimation*, Academic, San Diego, Calif.

Bencala, K. E., and R. A. Walters (1983), Simulation of solute transport in a mountain pool-and-riffle stream: A transient storage model, *Water Resour. Res.*, 19, 718–724.

Bencala, K. W., R. E. Rathbun, A. P. Jackman, V. C. Kennedy, G. W. Zellweger, and R. J. Avanzino (1983), Rhodamine WT dye losses in a mountain stream environment, *Water Resour. Bull.*, 19, 943–950.

Bradford, J. H., J. P. McNamara, W. B. Bowden, and M. N. Gooseff (2005), Imaging depth-of-thaw beneath Arctic streams using ground-penetrating radar, *Hydrol. Processes*, 19, 2689–2699.

Brosten, T. R., J. H. Bradford, J. P. McNamara, J. P. Zarnetske, M. N. Gooseff, and W. B. Bowden (2006), Profiles of temporal thaw depths beneath two Arctic stream types using ground-penetrating radar, *Permafrost Periglacial Processes*, 17, 341–355.

Collier, K. J., A. E. Wright-Stow, and B. J. Smith (2004), Trophic basis of production for a mayfly in a North Island, New Zealand, forest stream: Contributions of benthic versus hyporheic habitats and implications for restoration, *N. Z. J. Mar. Freshwater Res.*, 38, 301–314.

D'Angelo, D. J., J. R. Webster, S. V. Gregory, and J. L. Meyer (1993), Transient storage in Appalachian and Cascade mountain streams as related to hydraulic characteristics, *J. N. Am. Benthol. Soc.*, 12, 223–235.

Dingman, S. L. (1984), *Fluvial Hydrology*, pp. 121–136, W. H. Freeman, New York.

Edwardson, K. J., W. B. Bowden, C. N. Dahm, and J. Morrice (2003), The hydraulic characteristics and geochemistry of hyporheic and parafluvial zones in Arctic tundra streams, North Slope, Alaska, *Adv. Water Resour.*, 26, 907–923.

Elliott, A. H., and N. H. Brooks (1997), Transfer of nonsorbing solutes to a streambed with bed forms: Laboratory experiments, *Water Resour. Res.*, 33, 137–152.

Findlay, S., D. Strayer, C. Goumbala, and K. Gould (1993), Metabolism of stream water dissolved organic carbon in the shallow hyporheic zone, *Limnol. Oceanogr.*, 38, 1493–1499.

Fisher, H. B., J. E. List, C. R. Koh, J. Imberger, and N. H. Brooks (1979), *Mixing in Inland and Coastal Waters*, 302 pp., Elsevier, Netherlands.

Gooseff, M. N., D. M. McKnight, W. B. Lyons, and A. E. Blum (2002), Weathering reactions and hyporheic exchange controls on stream water chemistry in a glacial meltwater stream in the McMurdo Dry Valleys, *Water Resour. Res.*, *38*(12), 1279, doi:10.1029/2001WR000834.

Gooseff, M. N., S. M. Wondzell, R. Haggerty, and J. Anderson (2003), Comparing transient storage modeling and residence time distribution (RTD) analysis in geomorphically varied reaches in the Lookout Creek basin, Oregon, USA, *Adv. Water Resour.*, *26*, 925–937.

Grimm, N. B., and S. G. Fisher (1984), Exchange between interstitial and surface water: implications for stream metabolism and nutrient cycling, *Hydrobiologia*, *111*, 219–228.

Gucker, B., and I. G. Boechat (2004), Stream morphology controls ammonium retention in tropical headwaters, *Ecology*, *85*, 2818–2827.

Haggerty, R., and P. C. Reeves (2002), *STAMMT-L Version 1.0 User's Manual*, ERMS 520308, Sandia Natl. Lab., Albuquerque, N. M.

Haggerty, R., S. M. Wondzell, and M. A. Johnson (2002), Power-law residence time distribution in the hyporheic zone of a 2nd-order mountain stream, *Geophys. Res. Lett.*, *29*(13), 1640, doi:10.1029/2002GL014743.

Hamilton, T. D. (1986), Late Cenozoic glaciation of the Central Brooks Range, in *Glaciation in Alaska: The Geologic Record*, vol. 99, edited by T. D. Hamilton, K. M. Reed, and R. M. Thorson, pp. 9–49, Alaska Geol. Soc., Anchorage.

Hart, D. R., P. J. Mulholland, E. R. Marzolf, D. L. DeAngelis, and S. P. Hendricks (1999), Relationships between hydraulic parameters in a small stream under varying flow and seasonal conditions, *Hydrol. Processes*, *13*, 1497–1510.

Harvey, J. W., and K. E. Bencala (1993), The effect of streambed topography on surface-subsurface water exchange in mountain catchments, *Water Resour. Res.*, *29*, 89–98.

Harvey, J. W., and C. C. Fuller (1996), Effect of enhanced manganese oxidation in on basin-scale geochemical mass balance, *Water Resour. Res.*, *34*, 623–636.

Harvey, J. W., and B. J. Wagner (2000), Quantifying hydrologic interactions between streams and their subsurface hyporheic zones, in *Streams and Ground Waters*, edited by J. A. Jones and P. J. Mulholland, pp. 3–44, Academic Press, San Diego, Calif.

Harvey, J. W., M. H. Conklin, and R. S. Koelsch (2003), Predicting changes in hydrologic retention in an evolving semi-arid alluvial stream, *Adv. Water Resour.*, *26*, 939–950.

Kane, D. L., L. D. Hinzman, C. S. Benson, and G. E. Liston (1991), Snow hydrology of a headwater Arctic basin: 1. Physical measurements and process studies, *Water Resour. Res.*, *27*, 1099–1109.

Kasahara, T., and S. M. Wondzell (2003), Geomorphic controls on hyporheic exchange flow in mountain streams, *Water Resour. Res.*, *39*(1), 1005, doi:10.1029/2002WR001386.

Legrand-Marcq, C., and H. Laudelout (1985), Longitudinal dispersion in a forest stream, *J. Hydrol.*, *78*, 317–324.

Marquardt, D. W. (1963), An algorithm for least-squares estimation of nonlinear parameters, *J. Soc. Indust. Appl. Math.*, *11*(2), 431–441.

McNamara, J. P., D. L. Kane, and L. D. Hinzman (1997), Hydrograph separation in an Arctic watershed using mixing model and graphical techniques, *Water Resour. Res.*, *33*, 1707–1719.

Morrice, J. A., H. M. Valett, C. N. Dahm, and M. E. Campana (1997), Alluvial characteristics, groundwater-surface water exchange and hydrological retention in headwater streams, *Hydrol. Processes*, *11*, 253–267.

Osterkamp, T. E., and M. W. Payne (1981), Estimates of permafrost thickness from well logs in northern Alaska, *Cold Reg. Sci. Technol.*, *5*, 13–27.

Packman, A. I., and K. E. Bencala (2000), Modeling surface-subsurface hydrologic interactions, in *Streams and Ground Waters*, edited by J. A. Jones and P. J. Mulholland, pp. 45–80, Academic Press, San Diego, Calif.

Packman, A. I., and M. Salehin (2003), Relative roles of stream flow and sedimentary conditions in controlling hyporheic exchange, *Hydrobiologia*, *494*, 291–297.

Peterson, B. J., J. E. Hobbie, T. L. Corliss, and K. Kriet (1983), A continuous-flow periphyton bioassay: Test of nutrient limitation in a tundra stream, *Limnol. Oceanogr.*, *23*, 583–591.

Peterson, B. J., et al. (1993), Biological responses of a tundra river to fertilization, *Ecology*, *74*, 653–672.

Péwé, T. L., (1966), Ice-wedges in Alaska-classification, distribution, and climactic significance, in *Proceedings of the Permafrost International Conference*, NRC Publ. 1287, pp. 76–81, Natl. Acad. of Sci., Washington, D. C.

Pinder, G. F., and S. P. Sauer (1971), Numerical simulation of flood-wave modification due to bank-storage effects, *Water Resour. Res.*, *7*, 63–70.

Runkel, R. L. (1998), One-dimensional transport with inflow and storage (OTIS): A solute transport model for streams and rivers, *U. S. Geol. Surv. Water Resour. Invest. Rep.*, *98-4018*, 73 pp.

Sturm, M., T. Douglas, C. Racine, and G. E. Liston (2005), Changing snow and shrub conditions affect albedo with global implications, *J. Geophys. Res.*, *110*, G01004, doi:10.1029/2005JG000013.

Triska, F. J., J. H. Duff, and R. J. Avanzino (1990), Influence of exchange flow between the channel and hyporheic zone on nitrate production in a small mountain stream, *Can. J. Fish. Aquat. Sci.*, *47*, 2011–2099.

Vervier, P., M. Dobson, and G. Pinay (1993), Role of interaction zones between surface and ground waters in DOC transport and processing: considerations for river restoration, *Freshwater Biol.*, *29*, 275–284.

Wohl, E., et al. (2005), River restoration, *Water Resour. Res.*, *41*, W10301, doi:10.1029/2005WR003985.

Wondzell, S. M. (2006), Effect of morphology and discharge on hyporheic exchange flows in two small streams in the Cascade Mountains of Oregon, USA, *Hydrol. Processes*, *20*, 267–287.

Wondzell, S. M., and F. J. Swanson (1996), Seasonal and storm dynamics of the hyporheic zone of a 4th-order mountain stream: I. Hydrologic processes, *J. N. Am. Benthol. Soc.*, *15*, 3–19.

Wörman, A., A. I. Packman, H. Johansson, and K. Jonsson (2002), Effect of flow-induced exchange in hyporheic zones on longitudinal transport of solutes in streams and rivers, *Water Resour. Res.*, *38*(1), 1001, doi:10.1029/2001WR000769.

Zaramella, M., A. I. Packman, and A. Marion (2003), Application of the transient storage model to analyze advective hyporheic exchange with deep and shallow sediment beds, *Water Resour. Res.*, *39*(7), 1198, doi:10.1029/2002WR001344.

————————————

W. B. Bowden, Rubenstein School of the Environment and Natural Resources, University of Vermont, Burlington, VT 05401, USA.

J. H. Bradford, T. R. Brosten, and J. P. McNamara, Department of Geosciences, Boise State University, Boise, ID 83725, USA.

M. N. Gooseff, Department of Geology and Geological Engineering, Colorado School of Mines, Golden, CO 80401, USA.

J. P. Zarnetske, Department of Geosciences, Oregon State University, 104 Wilkinson Hall, Corvallis, OR 97331, USA. (zarnetsj@geo.oregonstate.edu)